A Preliminary Study of MM5 3D-VAR Initialization toward the Improvement of Weather Prediction

[1]Ching-Yuang Huang, [2]Ying-Hwa Kuo and [2]Wei Huang
[1]Department of Atmospheric Sciences, National Central University
[2]National Center for Atmospheric Sciences

Abstract

The recently developed MM5 3D-VAR system in NCAR has been used to investigate the influence of ingested data on short-term weather forecast. In this study, three weather events are investigated with the main focus on rainfall prediction, which include a Mei-Yu front on 06/1998 and Bilis super-typhoon on 08/2000 and Nari typhoon on 09/2001. With 3D-VAR, the simulated low pressure system extending off northeast of Taiwan for the Mei-Yu front event is stronger than that without 3D-VAR. The 24-h predicted heavy rainfall just off southern Taiwan and the propagation of the cut-off low center are also closer to the observed in the 3D-VAR run. In the second case of Bilis typhoon, both the runs with and without 3D-VAR show a northward track bias just upstream of eastern Taiwan as the initialization starts earlier on 0000Z/21/08/2000 about 39 h prior to landfall. However, even in this biased track, the 3D-VAR run still gives slightly better rainfall distribution as compared to the one without 3D-VAR. The bias of northward track deflection is reduced when the initialization time is put forward by 24 h.

The simulated Nari typhoon event starting from 0000Z/15/09/2001 first shows a right southwestward direction toward Taiwan during the earlier times but then makes a curved turn away off Taiwan afterward. When the initialization time is delayed by one day, the typhoon center does migrate continuously southwestward and makes a landfall on northern Taiwan but then stalls near the northwestern coastal region for some time. It was found that cloud convection is significantly enhanced as the vortex core is pushed to confront with the leading edge of Central Mountain Range (CMR) and is slowed down to rotates about the left side of CMR. The combination of compression and stagnation of the embedded convective system along CMR may explain the very large rainfall intensity in northwestern Taiwan. The feature of the observed large rainfall in the southwestern region off CMR is also captured but its intensity is significantly underpredicted due to lagging or weakening of the vortex center at later times in the runs with or without 3D-VAR. With the 3D-VAR, the simulated track is considerably improved, but the associated rainfall patterns remain similar. Several 3D-VAR initializations with a bogus vortex are attempted for the improvement of the rainfall prediction and will be reported in the conference.

1. Introduction

Data assimilation has recently recognized as a mean of providing better "consistent" initial conditions for numerical weather prediction in the meteorological community. One of the most attractive and effective methods is the utilization of estimation theory that provides a theoretical basis for variational analyses to minimize the bias of analysis data. This treatment through the so-called Kalman filter may provide theoretically best or "optimal" solution for the system to be analyzed (Zou et al., 1997). A full set of data in all assimilation time window has the beneficial impact resulted from the strong constraint upon the model integrated state with both physics and dynamics and is well known as 4D-VAR, which, however, is very time-consuming due to the adjoint nature in iteratively searching for the optimal solution. The degraded 3D-VAR which utilizes both the observations and analyses at the current time (i.e., the "initial time") and greatly simplifies the filtering process subject to the cheaper adjoint operator for the ingestion of observations (Vandenberghe and Kuo, 1999). Another advantage of the 3D-VAR, as compared to 4D-VAR, is the mathematic configuration on multi-domains which facilitate nested simulations for small-scale phenomena. With more and more conventional and unconventional data (including satellite, radar and other remote sensors), ingestion of these data into the NWP model has been believed to one of the top priorities toward the improvement on weather forecast. In practice, whenever these data become available, they should be assimilated during their ingestion time window provided their error covariance matrices have been well known. In this study, we utilize MM5 3D-VAR to incorporate sounding observations with the diagonal error covariance matrix provided by NCEP for the operation Spectral Statistical

Interpolation 3D-VAR system (Parrish and Derber, 1992). The details of the MM5 3D-VAR system can be found in Vandenberghe and Kuo (1999).

The performance of the MM5 3D-VAR is being under improvement with more types of observations included. This paper is a preliminary investigation of the current 3D-VAR system for conventional sounding observations. The goal of such a research is a realization of the most common sources for the operational need for which assimilation of remote sensing data is still not well developed or remains under testing.

2. Numerical setups

In this study, three cases were investigated, which include the Mei-Yu front cast (IOP-2 of SCSMEX) on 06/1998 and Bilis super-typhoon on 08/2000 and Nari typhoon on 09/2001. All the cases have been simulated by MM5 version 3.4 with ice/graupel physics in the finest domain and Grell's scheme for cumulus parameterization in outer domains and the Blackadar PBL parameterization in all the domains. Here is a brief summary for some model setups:

Mei-Yu front case: Two domains (45 and 15 km resolutions), 72 h forecast.

Bilis typhoon case: Three domains (45, 15 and 5 km resolutions), 60 h or 36 h forecast.

Nari typhoon case: Three domains (45, 15 and 5 km resolutions), 72 h or 96 h forecast

All the three cases will be simulated with and without 3D-VAR. The Nari typhoon simulation will also be targeted on the effectiveness of initial vortex bogusing methods, which mainly rely on 3D-VAR modulation rather than any conventional surgery method that implants a bogus vortex to replace the analyzed typhoon circulation. The results will be presented in the conference. In this paper, the mechanisms for enormous rainfall of Nari in the western and northern Taiwan will be discussed.

All the simulations have performed the MM5 objective module, LITTLE_R, to include the sounding observations, which have also been used in NCEP global assimilated analyses as the first guess data. Hence, the 3D-VAR initialization may be regarded as enhancement of the observational influence through the optimal Kaman filter. To some extent, the 3D-VAR approach is similar to optimal interpolation but has greater potential in the assimilation of unconventional data that are not directly predicted by the model. As more data are ingested into the model, the influence of the data assimilation processes on improving initial conditions may be expected.

3. The results

The first case is of typical Mei-Yu front that has migrated offshore at 0000Z/03/06/1998 and is aligned roughly across the mid-Taiwan and extended to southern Japan with an embedded low as can be seen in surface weather maps. This frontal structure in the vicinity of Taiwan is well captured in the model initial condition as shown in Fig. 1. A low-pressure system is being under development near the coastal region of northeastern Taiwan as the front is nearly stagnant in Taiwan and is somewhat distorted 24 h later. The weak surface low then northeastward migrates toward Japan with time and develops to a prominent cut-off low-pressure system just southeast of Japan after 72 h.

As can seen in Fig. 2, the 3D-VAR run has slightly stronger initial wind than the run without 3D-VAR, in particular, northeast of Taiwan. Although the initial difference seems to be minor, the 3D-VAR run produces a stronger low northeast of Taiwan at 24 h and is about 7 mb more deepening than that for the run without 3D-VAR at 36 h. After 72 h, both runs have exhibited a considerably biased propagation of the surface low but their simulated flow structures in this domain are similar. With stronger convergence and confluence, the 3D-VAR run also gives considerably larger rainfall (maximum 500 mm within 6 h) in the fine domain. The observed precipitation indicates that the east-west alignment of the rainband just off southern Taiwan in the 3D-VAR run is more consistent. The large difference in the rainfall distribution and intensity seems to strengthen the importance of the observation ingestion in the vicinity of the developing system and indicate the sensitivity of model prediction to such a small variation in the initial conditions.

The same testing on model initialization is further extended to the Bilis typhoon case that has also been simulated by Lin et al. (2001) using COAMPS. Both no-3DVAR and 3D-VAR runs are initialized at 0000Z/21/08. As seen in Fig. 3, the initial analyses for both cases are very similar everywhere expect for the surface low pressure in southern China and some minor difference in oceanic regions. For example, a noticeable feature is seen in the 1008-mb pressure contour that crosses Taiwan only in the analyses of the 3D-VAR run. The initialized surface low pressure for Bilis is only 997 mb for both the runs, indicating a demand of vortex bogusing.

After 36 h, Bilis has deepened to 966 mb (without 3D-VAR) and 969 mb (with 3D-VAR) and hence the former has slightly stronger near-surface wind. At this time, a low center of 930 mb was observed for Bilis prior to a landfall

3 h later. Both the runs appear to produce biased (lagged) tracks with northward deflection since the observed track at this time is southwest of the predicted. The movement of the typhoon center for the no-3DVAR run is slightly faster but is more biased in position than for the 3D-VAR run as seen in the 36 h forecast of Fig. 4. At 39 h, the 3-h accumulated rainfall is generally greater for the no-3DVAR run as shown in Fig. 5. For example, the peak rainfall south of I-Lan is 147 mm for the no-3DVAR run compared to 101 mm for the 3D-VAR run. Moreover, the large rainfall for the no-3DVAR run is also distributed too southward as well as inland as compared the observed (not shown). The northward track bias is reduced as the initial time is put forward 24 h as seen in Fig. 5. However, the predicted low center is only 977 mb at the same time for only 15 h model integration. Hence, the predicted rainfall intensity is slightly weaker than the previous two runs but the associated rainfall distributions are more similar to those of the 3D-VAR run, probably due to their more coherent tracks.

The simulation results for the typhoon case also indicate the importance of a realistic feature of the initial typhoon circulation and therefore certainly demands vortex bogusing to well represent the observed intensity. Before a complete surgery as performed in several numerical models, the 3D-VAR minimization may still be feasible to spin up the vortex through some prescribed ship observations for surface pressure and wind. We have tried to reset the analyzed and "observed" sea-surface pressure at the typhoon center to lower values, e.g., 975 mb and find that there is little improvement in the enhancement of initial typhoon circulation (not shown). Another bogus method by prescribing more data including the observed Quickscat wind is being under the way. The research once upon completion will be reported in the conference.

The simulation of Nari typhoon in 2001 is mainly focused on the rainfall mechanisms responsible for the enormous intensity occurred in northern and western Taiwan. A sensitivity test of the initial time indicates that the forecast if started on 0000Z/15/09 does show a slow southwestward movement toward Taiwan during the first two ways but then makes a curved turn away from Taiwan afterward. On the other hand, it was found that NCEP global model (AVN) prediction is able to exhibit a landfall on northeastern Taiwan but with a following wrong track at the different side along eastern Taiwan. As the initial time is lagged to 0000Z/16/09 (one day later), the simulated Nari typhoon center is able to make a landfall at northern Taiwan. The evolving typhoon vortex is depicted in Fig. 6. After 12 h, the surface low center already strengths to 986 mb and is producing stronger upslope flow passing the northern edge of CMR. The along-slope contours of rainfall in Fig. 7a tend to confirm this mechanism. There is a prominent peak rainfall just on the Tar-Tun Mountain at the northern tip, which is associated with intense upslope flow of the inner vortex core and is believed to be also in response to the intensifying cloud convection as stagnated by topographic blocking. More analyses, however, need to be done in order to distinguish the relative importance of the above two mechanisms.

As the vortex core moves to the northern coast nearby Tan-Sui, the upslope flow in the vicinity of the Tar-Tun Mountain disappears and migrates to further southern regions (Fig. 6b). As a consequence, the location of peak rainfall also moves southward and extends roughly along the western slope. The major rainfall disappears outside the intense vortex circulation and in the lee side of CMR, indicating that the major mechanism for the rainfall may be due to the enhancement of the cyclonically rotating rainband as it confronts with the steep topography (Fig. 6b and 7b). At 24 h, the simulated vortex center moves southwestward and the upslope flow is less prominent over CMR. Note that the peak rainfall doesn't occur near the steepest slope and its geometric distribution now is in north-south alignment. As can be clearly seen, the inland flow of the vortex core near the northwestern coastal region is suddenly compelled into the topographically blocked flow associated with the previously existent rainbands. This convergent process may produce upward motions and provide abundant moisture flux for rainfall enhancement.

At 36 h, the upslope flow disappears completely as the vortex center moves slightly southwestward. As a result, the rainfall intensity during 30-36 h is much weaker. The vortex center, however, does not continuously move southward by 48 h but instead appears to be slightly westward just off the coast. This offshore movement allows more upslope in mid-CMR and results in the large rainfall in Char-Yi. For another 24 h later, the vortex center is able to move southward to Tai-Chung and the rainfall band also extends more southward consequently. The CWB best track indicates that the low center is slightly offshore of Kuoshiang on 0000Z/19/09. At this time, the simulated surface low has weakened to 997 mb and is close to the observed.

The runs with and without 3D-VAR actually have almost identical initial analyses in the third domain (not shown). However, the simulated track is improved with 3D-VAR as seen in Fig. 8. For example, the landfall position now is quite close to the observed but with a slightly weakened surface center (990 mb) as compared to that without 3D-VAR. Also, the vortex keeps a

southwestward movement with time by 48 h. The vortex is somewhat less organized as it moves along the western side of the CMR and produces more inland and upslope flow. Despite these discrepancies in the vortex's displacement and movement, the large rainfalls at northern Taiwan and middle western Taiwan are presented in the 3D-VAR run as well.

It doesn't seem to indicate that MM5 has well simulated the observed important features of the intense rainfall in southwestern Taiwan since it is considerably underpredicted and the time phase is also not coherent due to lagging or weakening of the vortex center. Indeed, CWB observations tend to evidence a second strengthening of the vortex as it nearly stagnates in the western coastal region. This enhancement of the vortex should be the major mechanism for the enormous rainfall in Char-Yi and such a rainfall simulation could render a big challenge for any forecast model. But, as a result, the simulated geometric distribution of total accumulated rainfall during 72 h integration time is similar to the observed pattern, rendering about a maximum of 700 mm in the northern tip of Taiwan and a maximum of 500 mm in middle western Taiwan.

4. Conclusions

The MM5-3DVAR is being under development in NCAR and has a great potential in the improvement of weather forecast due to optimal initial analyses by taking many types of observations into assimilation. It may also provide an analysis tool for the adjustment of a bogused vortex through the minimization of the Kalman filer. We have examined the performance of MM5 3D-VAR in three cases (one for Mei-Yu front and two for typhoons). The limited evidences from the above case study may not substantially assert the effectiveness of 3D-VAR but the presented more coherence has indicated the great sensitivity of the model performance to the initial conditions when the influence of observations is further modulated through the optimization process of 3D-VAR. We will continue to ingest remote sensing data (e.g., precipitable water and Quickscat wind) to resolve the typhoon vortex and further expose the potential of 3D-VAR initialization as the dynamic constraint is included to modulate the vortex structure. In contrast to 4D-VAR in which the analysis data always stick to the model adjoint state and thus are dynamically more consistent and effective, efficient 3D-VAR optimization only has a weak constraint on balanced flow approximation and its effectiveness for vortex bogusing is worthy of more investigations.

References

Lin, Y.-L, D. B. Ensley, S. Chiao, C. M. Hill and C.-Y. Huang, 2001: Orographic influences on rainfall and track deflection associated with the passage of a tropical cyclone. Submitted to *Monthly Weather Review*.

Parish D. and J. Derber, 1992: The National Meteorological Center Spectral Statistical Interpolation analysis. *Monthly Weather Review*, **120**, 1747-1763.

Vandenberghe, F. and Y.-H. Kuo, 1999: Introduction to the MM5 3D-VAR Data Assimilation System: Theoretical Basis. NCAR/MMM documents, 38 pp.

Zou X., F. Vandenberghe, M. Pondeca, Y.-H. Kuo: Introduction the Adjoint Techniques and the MM5 Adjoint Modeling System. NCAR Technical note, NCAR/TN-435-STR, available from NCAR.

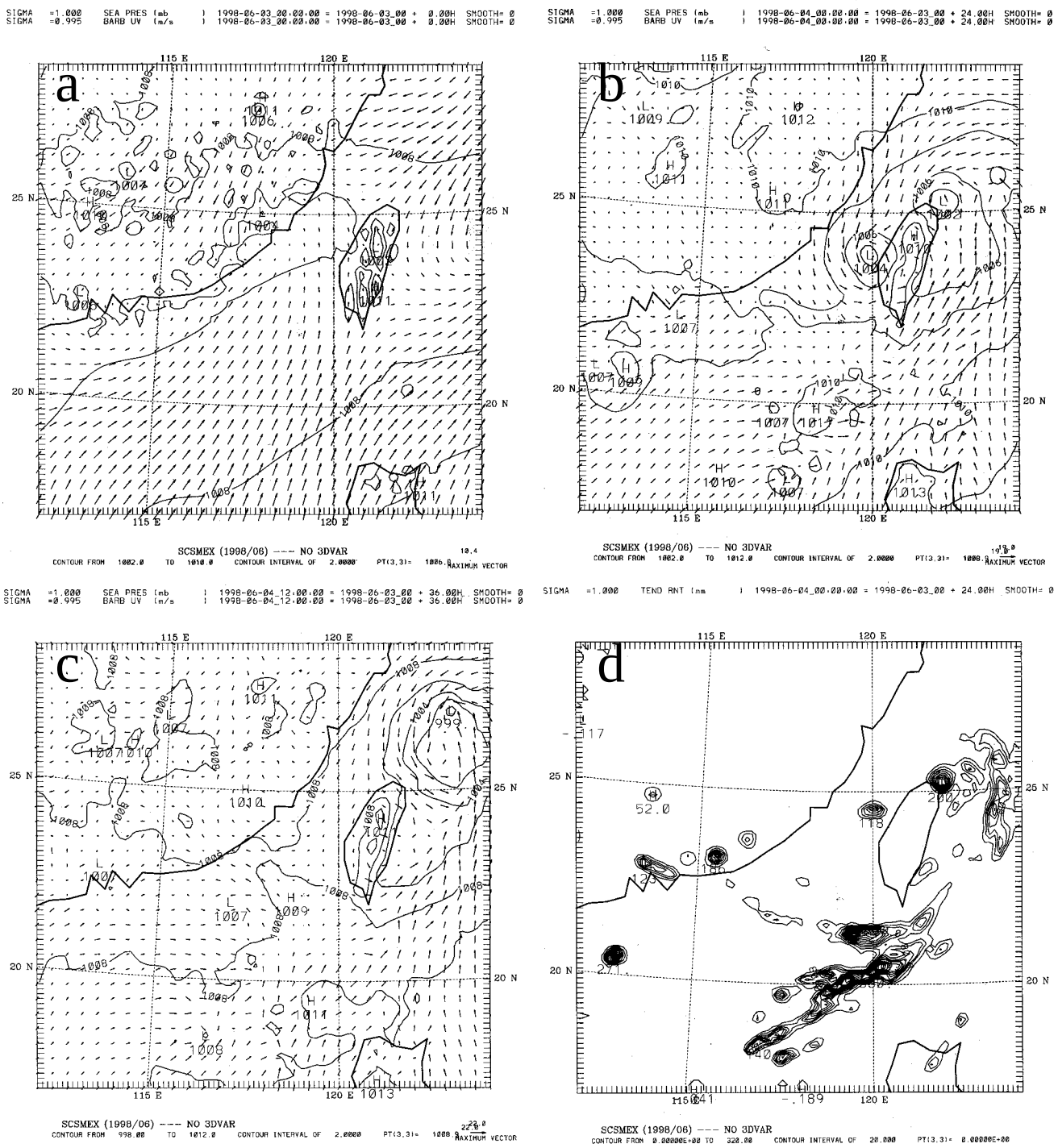

Fig. 1. The simulated sea-level pressure and near-surface wind in the second domain without 3D-VAR for the Mei-Yu front case in 1998 for (a) the initial time, 0000Z/03/06, (b) 24 h forecast, (c) 36 h forecast. (d) as in (b) but for the 6 h accumulated rainfall amount during 1800Z/03/06~0000Z/04/06 with contour interval of 20 mm.

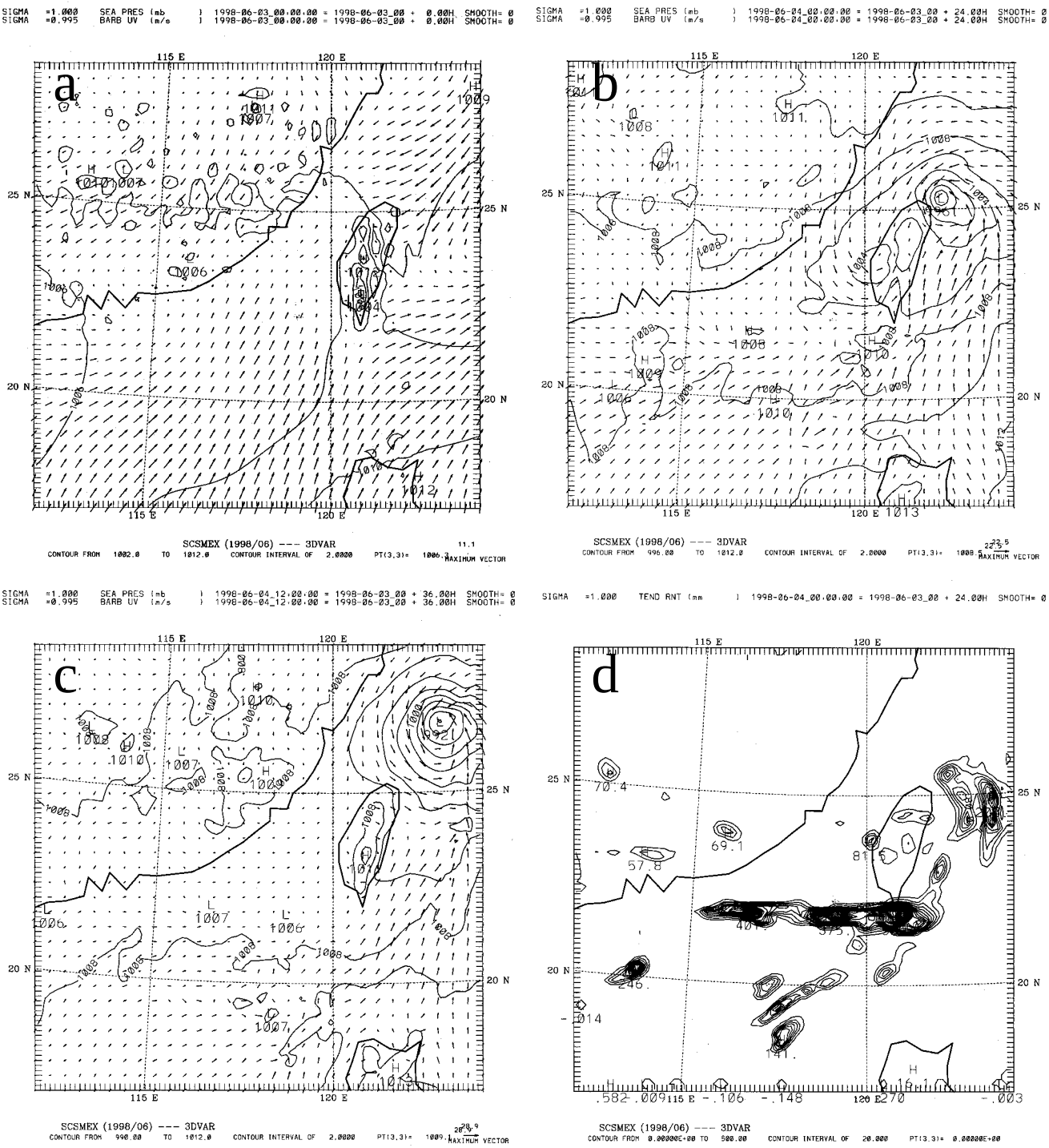

Fig. 2. As in Fig. 1 but for the initialization with 3D-VAR.

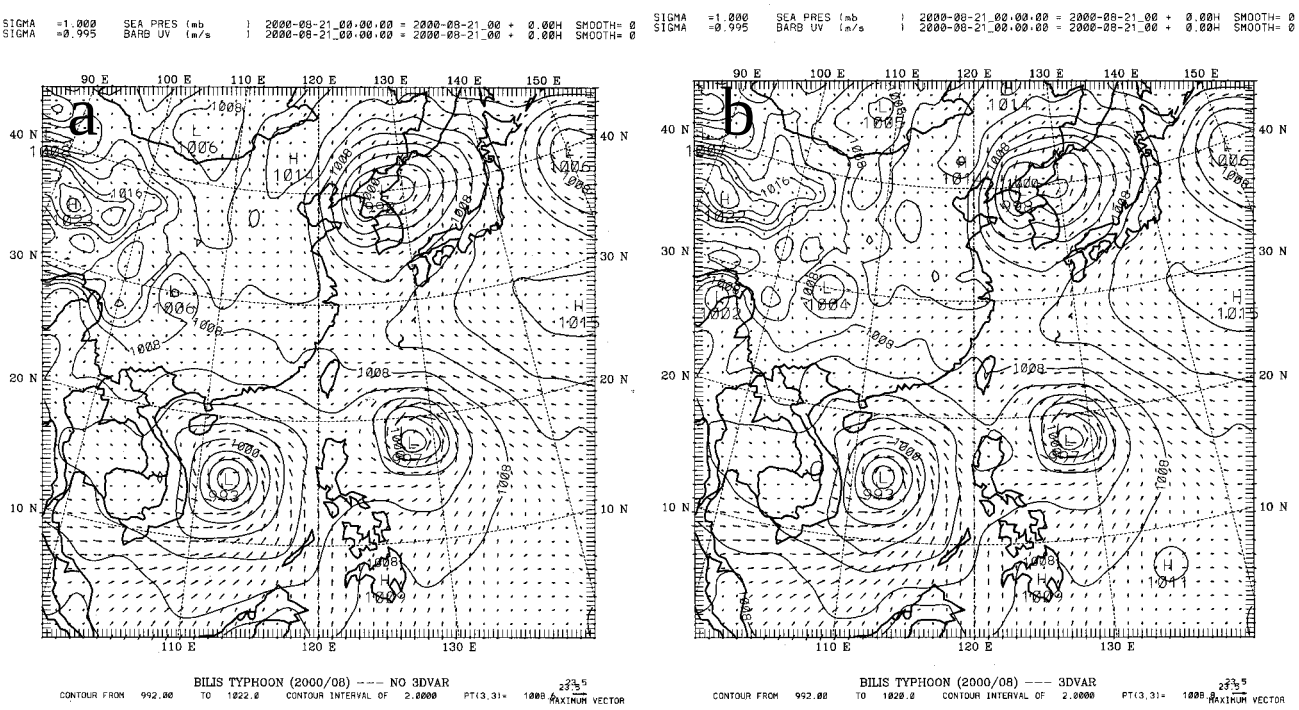

Fig. 3. The sea-level pressure and near-surface wind in the first outer domain for Bilis typhoon case in 2000 at the initial time at 0000Z/21/08 for the runs (a) without 3D-VAR and (b) with 3D-VAR.

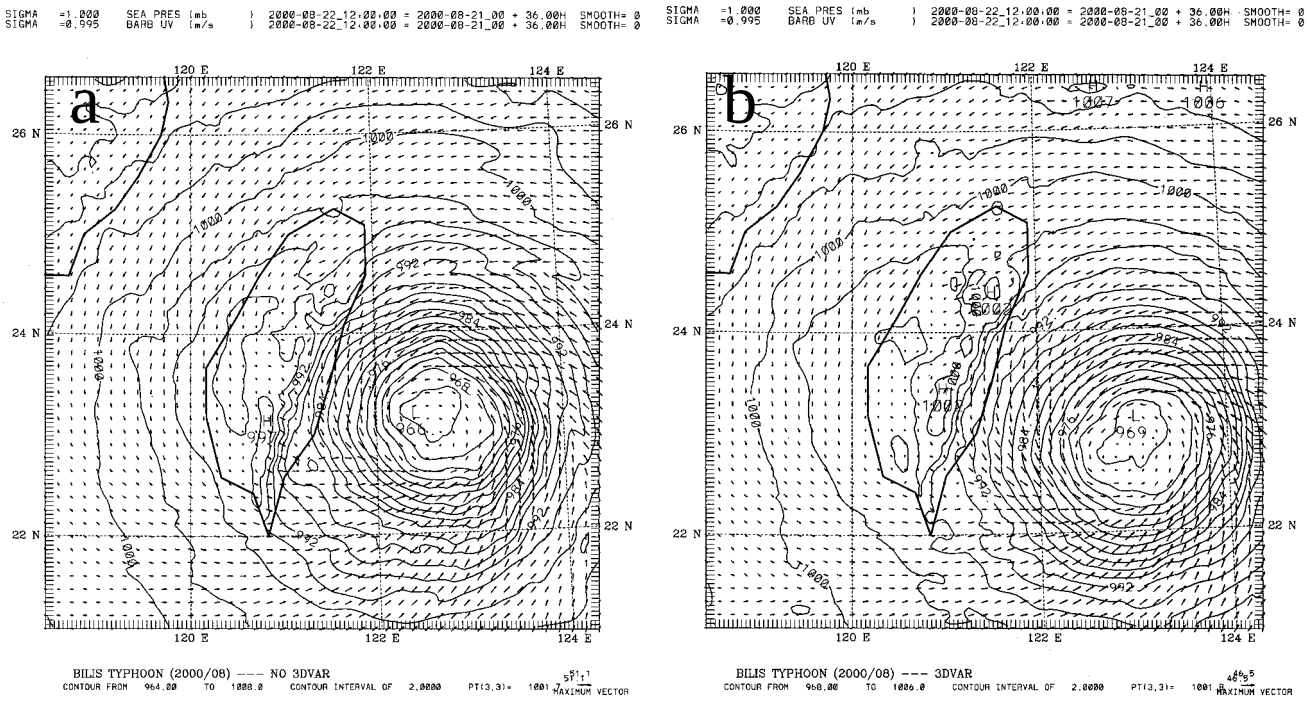

Fig. 4. As in Fig. 3 but for 36 h forecast.

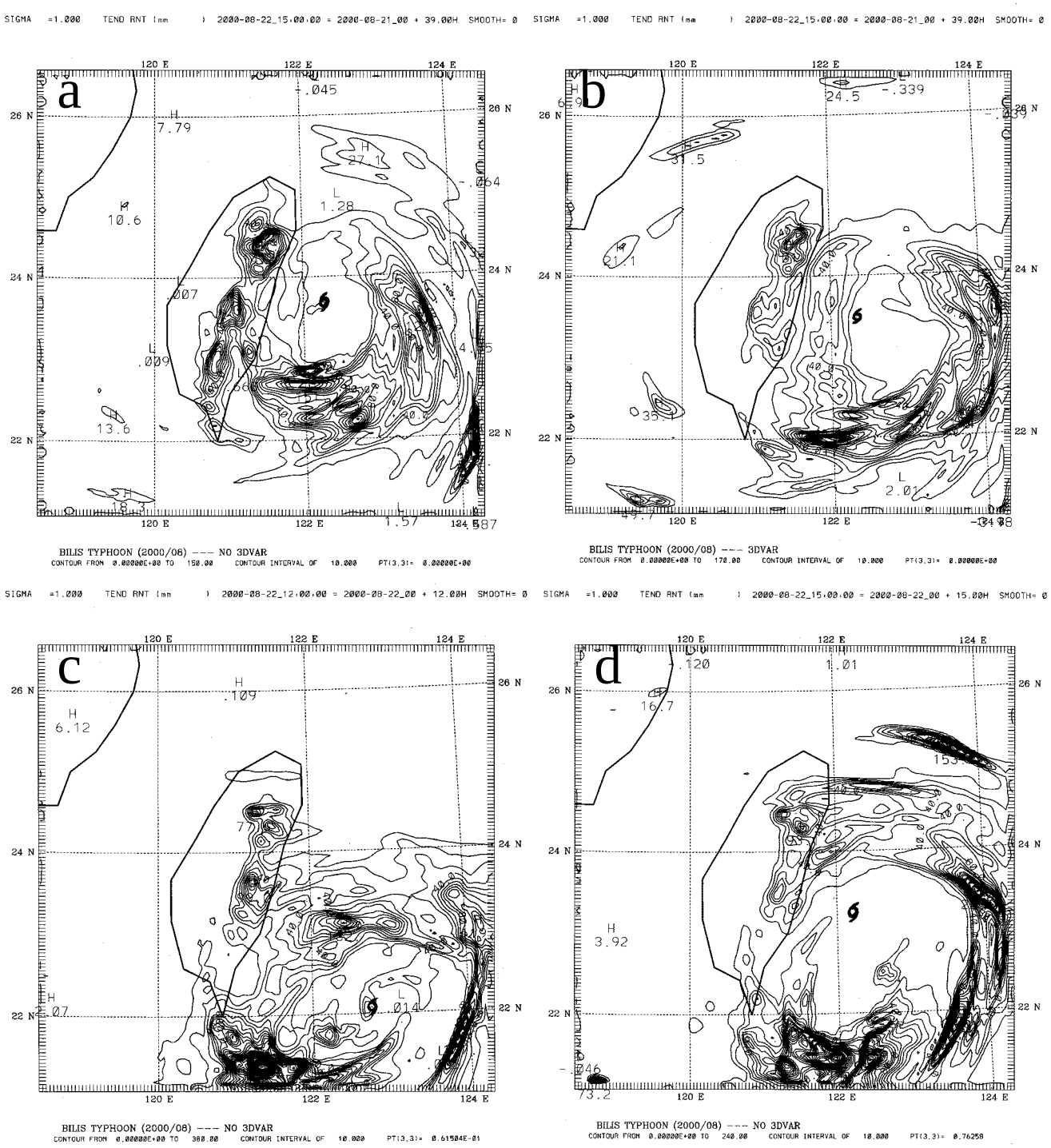

Fig. 5. The accumulated rainfall amount for the Bilis typhoon case in 2000 (a) during 1500Z/22/08~1800Z/22/08 for the run initialized at 0000Z/21/08 without 3D-VAR, (b) as in (a) but with 3D-VAR, (c) during 0900Z/22/08~1200Z/22/08 for the run initialized at 0000Z/22/08 without 3D-VAR and (d) as in (c) but during 1200Z/22/08~1500Z/22/08. Contour interval is 10 mm in all panels.

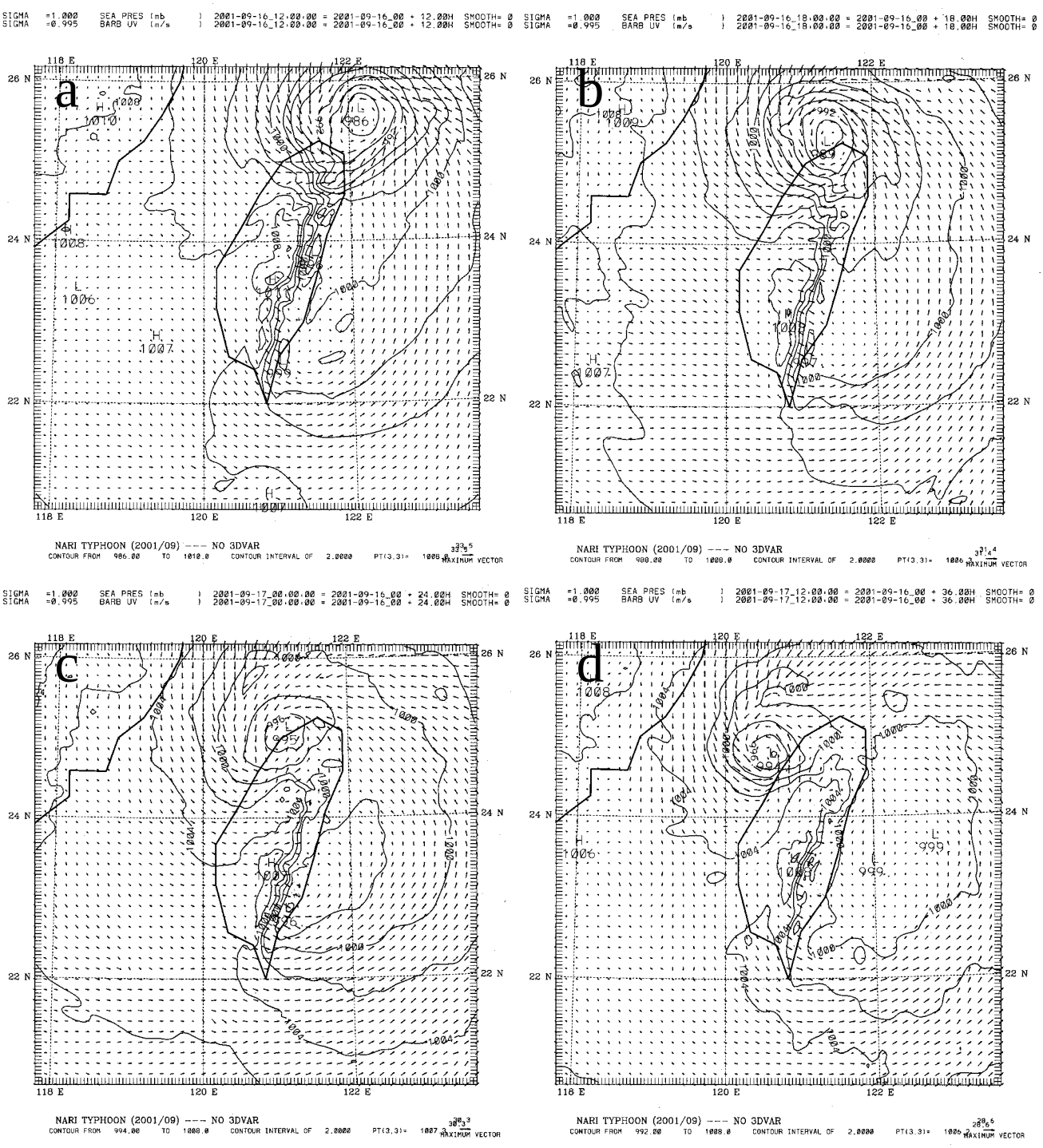

Fig. 6. The simulated sea-level pressure and near-surface wind in the third domain without 3D-VAR for the Nari typhoon case initialized at 0000Z/16/09/2001 for (a) 1200Z/16/09, (b) 1800Z/16/09, (c) 0000Z/17/09 and (d) 1200Z/17/09.

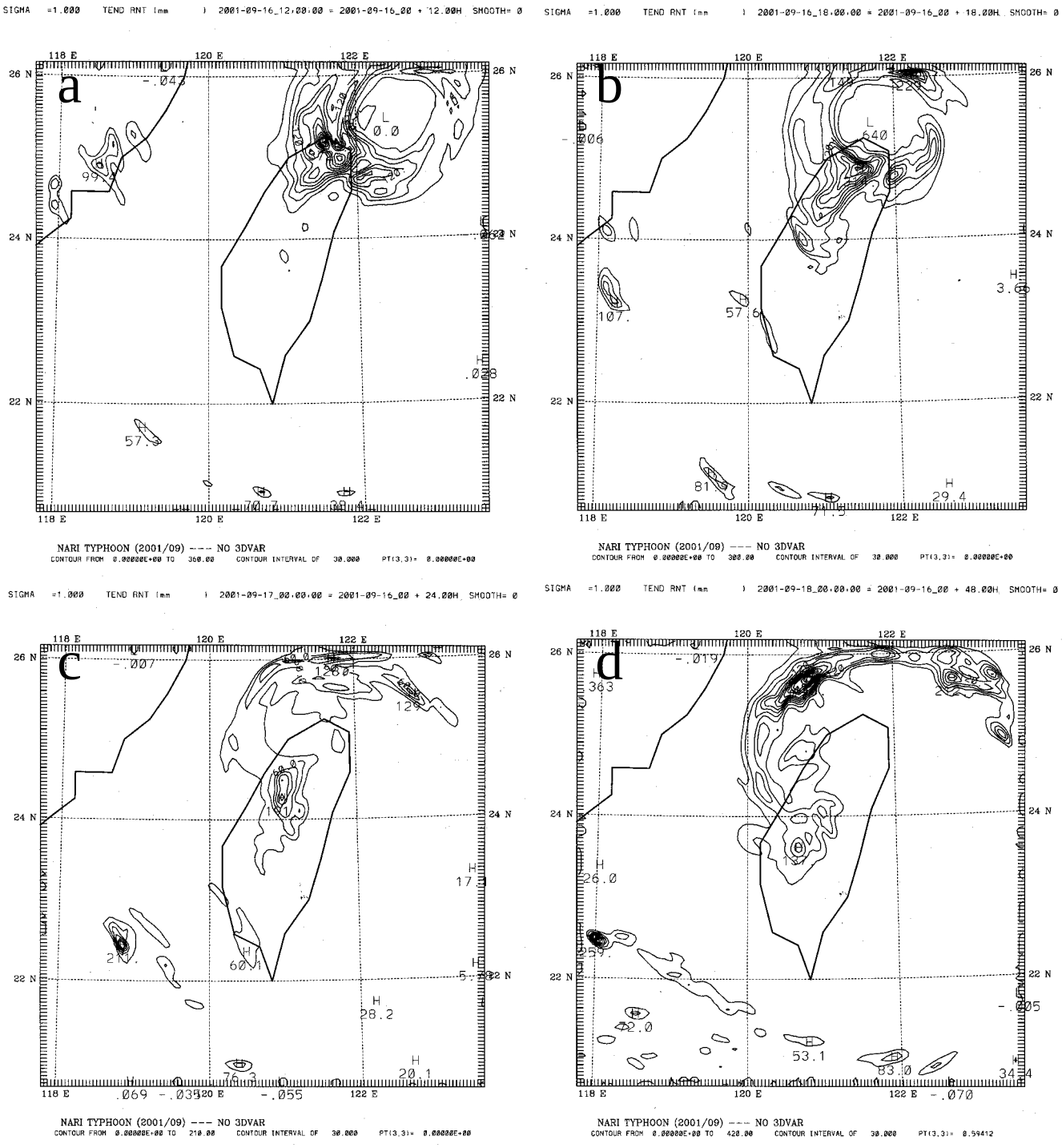

Fig. 7. The accumulated rainfall amount in the third domain without 3D-VAR for the Nari typhoon in 2001 during (a) 0600Z-1200Z/16/09, (b) 1200Z-1800Z/16/09, (c) 1800Z/16/09~0000Z/17/09, and (d) 1800Z/17/09~0000Z/18/09. Contour interval is 30 mm in all panels.

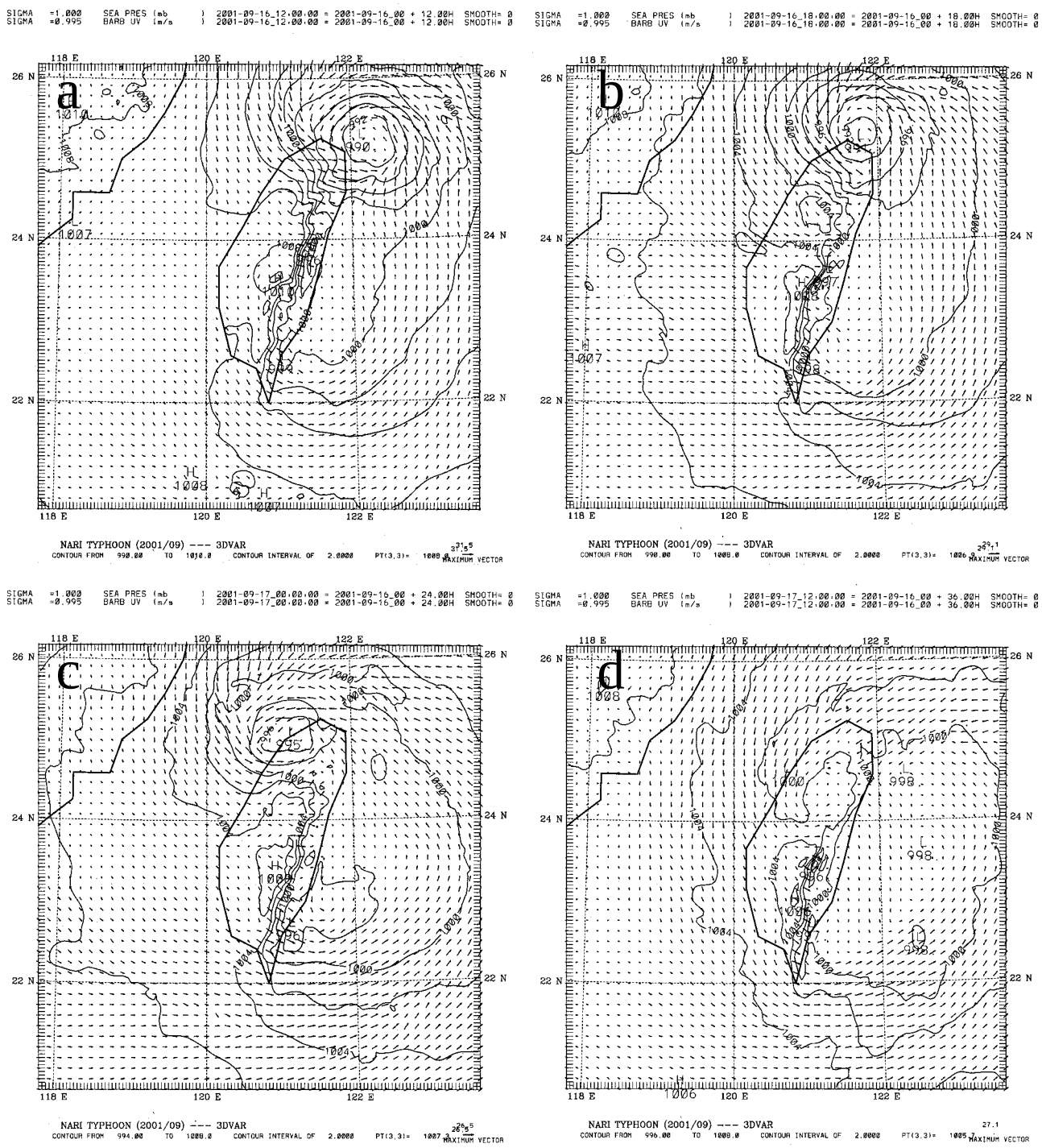

Fig. 8. As in Fig. 6 but for the run with 3D-VAR.

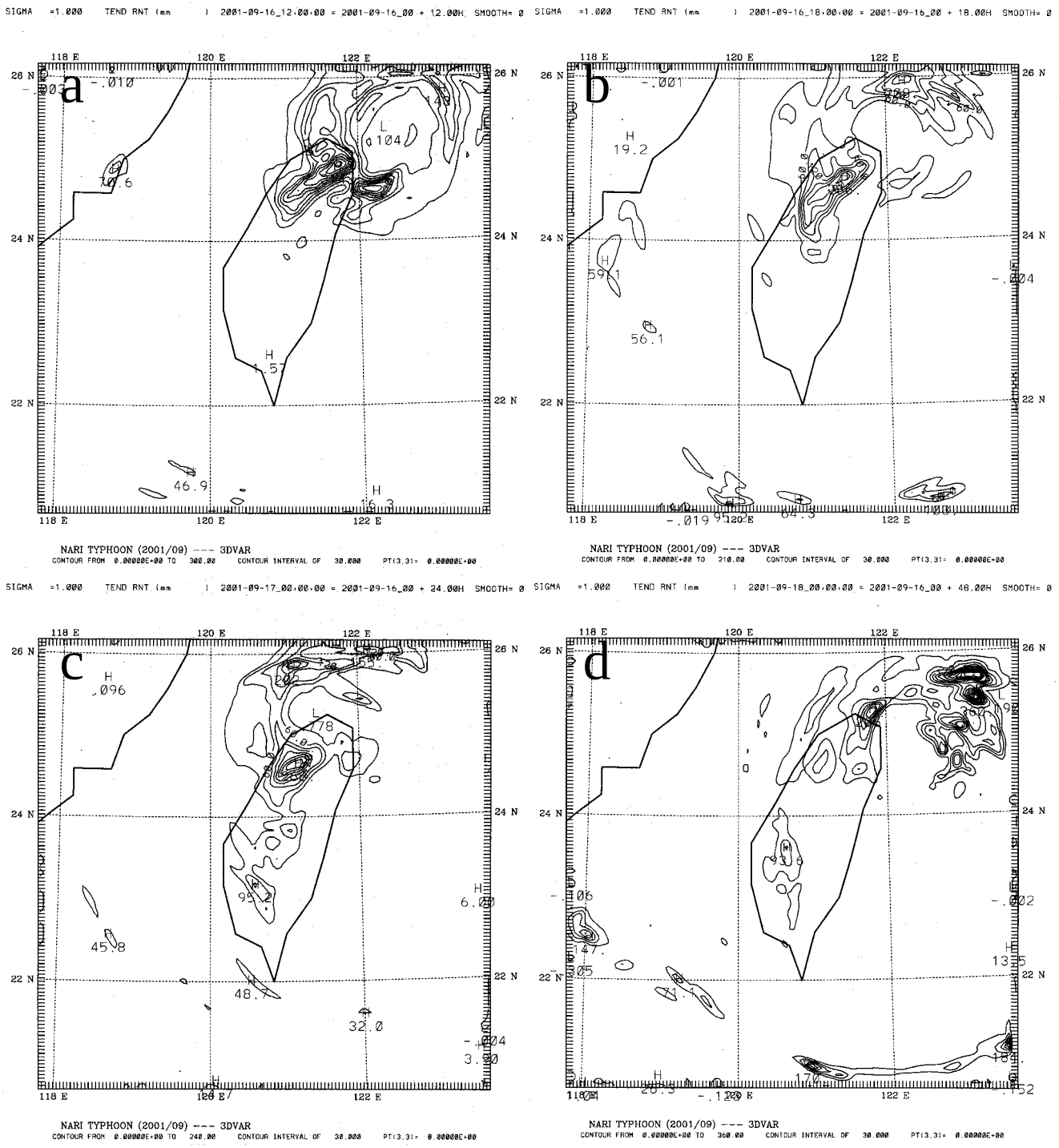

Fig. 9. As in Fig. 7 but for the run with 3D-VAR.